Morphological and Molecular Characteristics of Fungal Species Associated with Crown Rot of Strawberry in South Korea

Oliul Hassan
  Kyungpook National University

Taehyun Chang (✉ thchang@knu.ac.kr)
  Kyungpook National University   https://orcid.org/0000-0002-0213-7444

Abstract

Crown and root rot is the most important and destructive strawberry diseases in Korea as it causessubstantial economic loss. In August 2020, a severe outbreak of crown and root rot on strawberries (Fragaria×ananassa Duch.) was observed in the greenhouse at Sangju, South Korea. Infected plantlets displayed browning rot within the crown and root, stunted growth, and poor rooting. Thirty fungal isolates were procured from the affected plantlet. Isolates were identified based on morphological characteristics and pathogenicity test as well as sequence data obtained from internal transcribed spacer, large subunit ribosomal ribonucleic acid, translation elongation factor,and RNA polymerase Ⅱ-second largest subunit. Results showed that thecrown and root rot of strawberry in Korea was caused by three distinct fungal species:*Fusarium oxysporum* species complex, *F. solani* species complex, and*Plectosphaerella cucumerina*. To the best of our knowledge,*F. solani* species complex and*P. cucumerina*are reported for the first time as the causal agents of the crown and root rot of strawberryin South Korea.Pathogenicity tests confirmed that these isolates are pathogenic to strawberry.Understanding the composition and biology of the pathogen population will be helpful toprovide effectivecontrol strategies for the disease.

Introduction

Strawberry (*Fragaria × ananassa*) is cultivated across South Korea. South Korean strawberry is the most popular fruit due to its softness and sweetness. In South Korea, the cultivation of this fruit has increased rapidly in recent years. The cultivation area occupies 6435 hectares, and the total production is ~ 208,699 tons (Wei et al., 2020). With the expansion of growing areas and increase in output, many fungal diseases are posing a challenge to strawberry growers in South Korea. Among them, the crown and root rot in strawberry is the most important and destructive disease. It is also a common threat to commercial production of strawberry worldwide, including Australia, Bangladesh, and China (Fang et al., 2012; Gilardi et al., 2019; Surovy et al., 2019; Zhan et al., 2020). This disease limits plant growth and fruit production (Fang et al., 2012; Gilardi et al., 2019). The browning rot within the crown and root, stunted growth, and poor rooting are the typical manifestations in an infected plant (Park et al., 2019). Single or combinations of fungal and oomycete pathogens are responsible for this strawberry disease (Fang et al., 2012). *Fusarium oxysporum* and *Rhizoctonia* spp. are the frequently reported fungal species that cause crown and root rot of strawberry (Fang et al., 2011; Fang et al., 2012). Thus far, in South Korea, *Fusarium oxysporum* f. sp. *fragariae*, *Pythium* spp. *R. fragariae*, *R. solani*, and *Neopestalotiopsis clavispora* have been reported as the so-called crown and root rot of strawberry (KSPP 2009; Nam et al., 2020; Gilardi et al., 2019).

The causative agents of crown and root rot of strawberry were identified using the most traditional method (KSPP 2009; Gilardi et al,. 2019). The shape and size of the conidia and chlamydospores and culture characteristics were used in the conventional method. These criteria are not enough to delineate fungal species, especially species within the *Fusarium oxysporum* complex due to the following reasons: the fungal species complex share similar features and environmental factors that influence morphological characteristics (Taylor et al., 2000; Stewart et al., 2006). Molecular analysis along with morphological characteristics is a highly recommended approach for the precious identification of fungal species. Nam et al. (2020) described the genetic diversity of *F. oxysporum* f. sp. *fragariae* from strawberry in Korea using the nuclear ribosomal intergenic spacer region and translation elongation factor (*EF-la*) gene. They found that all the isolates of *F. oxysporum* f. sp. *fragariae* were formed of three clades in the phylogenetic tree. *EF-la* is an essential molecular marker that identifies most but not all fusaria (Geiser et al., 2004). O'Donnell et al., (2015) suggested DNA sequence-based identification of *Fusarium* using TEF-1, RNA polymerase II largest (RPB1), and the second largest subunit (RPB2) marker. *Fusariam* spp. needs to be identified using the recommended new gene marker.

According to the most of the grower from the Sangju region of South Korea, crown and root rot of strawberry has become more destructive and prevalent recently. The pathogens responsible for this disease in Sangju, Korea, have not been systematically investigated. Anxiety among the farmers is growing as the management strategies that were taken to contain this disease were not effective. One of the main reasons behind this could be the lack of proper diagnosis of the pathogen population. The sensitivity of fungi in different genera or different species within the same genus against a particular fungicide is not the same (Hellin et al. 2017; Ramdial et al. 2017). Hellin et al. (2017) found that *F. culmorum* is more sensitive to triazoles compared with *F. graminearum* and *F. cerealis*. *Cholletotrichum truncatum* isolated from bell paper is less susceptible to benomyl fungicide compared with *F. incarnatum-equiseti* species complex isolates (Ramdial et al., 2017). The identification of the pathogen population is essential to develop control strategies especially using fungicides.

This study aimed to identify the potential pathogens associated with the crown and root rot of strawberry in Sangju, Korea, characterized using a morphological and multigene approach. Moreover, this study aimed to confirm the pathogenicity of any recovered isolates.

Materials And Methods

Sample collection, pathogen isolation, and primary identification of pathogen population

Twenty-five affected strawberry plants showing wilting, collapse and root and crown rot were sampled from five greenhouses in Sangju, South Korea (Fig. 1). Crown was the more affected part compared with the root in these plants. The plants were propagated using the runner pegging method in a pot containing pasteurized soil and vermicompost. Plants were drip-irrigated with fertilizer mixed river water to adjust nutrients in the pot soil. Approximately 6 mm^2 tissue pieces were cut from the discolored area of the crown (Fig. 1D) of sampled plant, surface sterilized by dipping into 0.5% NaOCl solution for 1 min followed by 40 s in 70% ethanol, rinsed twice in sterile water, and then blot-dried with clean tissue paper. Tissue pieces plated on potato dextrose agar (PDA; Difco Becton Dickinson) were amended with 0.05 g/L tetracycline and incubated at room temperature (23°C ± 2°C) in the dark for 2–3 d. Hyphal tips of emerging hyphae were transferred to fresh PDA and were cultured for further use. A total of 30 pure fungal isolates were obtained and identified to genus level using morphological characteristics (Šišić et al.2018; Maryani et al. 2019; Zhang et al. 2019). For a long time, all the isolates were preserved as mycelium in 10% glycerin at −70°C. Then, pure culture repregenting identified each fungal species were deposited in the Korean Agricultural Culture Collection (KACC). (note: accession number will be assaign soon).

DNA extraction, PCR amplification, and sequencing

The fungal isolates from the strawberry plant were tentatively identified as *Fusarium* spp. and *Plectosphaerella* spp. based morphological criteria (Šišić et al., 2018; Maryani et al., 2019; Zhang et al., 2019). All the isolates of *Plectosphaerella* spp. shared the similar colony color, whereas some isolates of *Fusarium* spp. were pinkish-white and some were white. Four isolates *Plectosphaerella* spp. and nine isolates from *Fusarium* spp. (six pinkish-white and three white) were selected for species identification using the molecular approach. Actively growing cultures on PDA were used for DNA isolation. Genomic DNA was isolated using The HiGene Genomic DNA Prep Kit (BIOFACT, Yuseong-Gu, and Daejeon, Korea) following the instruction of the manufacturer and then stored at 4°C for further use.

Following four genes were selected for amplification and sequencing: the internal transcribed spacer (*ITS*) region and domains D1/D2/ D3 of the nuclear large subunit (*LSU*) rRNA, the translation elongation factor 1 alpha (*EF-1 a*), and the second largest subunit (*rpb2*). The selected genetic fragments (*ITS*, *LSU*, *EF-1 a*, and *rpb*2) were amplified with the primers listed in Table 1 using the PCRmax Alpha cyclers (PCR max, Stone, United Kingdom) in a total volume of 25 uL. The PCR mixture contained 2.5 μL F-star buffer, 0.5 μL dNTP Mix (each 10mM), 1 μL forward primer (10 pmol), 1 μL reverse primer (10 pmol), 1 μL template DNA, 0.2 μL F-star (*Taq* DNA polymerase), and 18.8 μL Invitrogen ultrapure DNase/RNase free distilled water. The PCR conditions for *ITS* were as follows: 4 min at 95°C, 30 s at 95°C, 30 s at 55°C (annealing), 45s at 72°C (34 cycles), and a final extension of 7 min at 72°C. The PCR conditions for *LSU*, *EF-1 a*, and *rpb*2 were almost similar to that of ITS except for the annealing temperature. The annealing temperature for *LSU*, *EF-1 a*, and *rpb*2 were 60°C, 56°C, and 59°C, respectively. To confirm successful PCR reactions, all resulting PCR products were visualized in 1.5% agarose gels (wt/v) stained with ethidium bromide and viewed under ultra-violet light. The products of the confirmed PCR reaction were purified using a HiGene PCR Purification Kit (Yuseong-Gu) as instructed by the manufacturer and sequenced in both directions directly with the help of Macrogen, Inc (Seoul, Korea). The resulting sequences were analyzed in SeqMan v.7.1 from the Lasergene package (DNASTAR, Inc.Madison, WI 53705 USA), edited manually whenever necessary, saved as a consensus sequence, and then deposited in the GenBank. The accession numbers of present and reference isolates are given in Table 2.

Table 1
List of primer sets used for amplification of selected genetic fragments.

Gene	Primer Name	Direction	Sequence (5'-3')	References
ITS	ITS-1	Forward	TCCGTAGGTGAACCTGCGG	White et al. (1990)
	ITS-4	Reverse	TCC TCC GCT TAT TGA TAT GC	White et al. (1990)
LSU	LROR	Forward	ACCCGCTGAACTTAAGC	Rehner and Samuels (1994)
	LR5	Reverse	TCCTGAGGGAAACTTCG	Vilgalys and Hester 1990
EF-1 α	EF1	Forward	ATGGGTAAGGARGACAAGAC	O'Donnell et al. (1998)
	EF2	Reverse	GGARGTACCAGTSATCATG	O'Donnell et al. (1998)
rpb1	RPB1-Fa	Forward	CAYAARGARTCYATGATGGGWC	O'Donnell et al. (2010)
	RPB1-G2R	Reverse	GTCATYTGDGTDGCDGGYTCDCC	O'Donnell et al. (2010)
rpb2	RPB2-5F2	Forward	GGGGWGAYCAGAAGAAGGC	O'Donnell et al. (2010)
	RPB2-7cR	Reverse	CCCATRGCTTGYTTRCCCAT	O'Donnell et al. (2010)

Table 2
GenBank accession numbers of fungal isolates used in this study.

Species	Isolates	Origin	Host	GenBank accession number			
				ITS	*EF-1 α*	*rpb2*	*LSU*
F. incarnatum-equiseti	NRRL45997	–	–		GQ505672	GQ505850	
F. longipes	NRRL20695	–			GQ915509	GQ915493	
F. mangiferae	UMAF 0924	–	*Mangifera indica*		KP753402	KP753442	
F. oxysporum f. sp.*conglutinans*	NRRL54008	Raphanus sp.	–		LS479673	LS479225	
F. oxysporum f. sp.*cubense*	FocCNPMF-R1	Brazil			LS479642	LS479196	
F. oxysporum f. sp.*lycopersici*	NRRL34936		*Solanum lycopersicum*		LS479646`	LS479200	
	NRRL 26381		*S. lycopersicum*		LS479641	LS479195	
F. oxysporum (present isolates)	SJB143	South Korea	*Fragaria* x *ananassa*	LC633891	LC633917	LC633930	LC633904
	SJB232	South Korea	*Fragaria* x *ananassa*	LC633892	LC633918	LC633931	LC633905
	SJB382	South Korea	*Fragaria* x *ananassa*	LC633893	LC633919	LC633932	LC633906
	SJB593	South Korea	*Fragaria* x *ananassa*	LC633894	LC633920	LC633933	LC633907
	SJB522	South Korea	*Fragaria* x *ananassa*	LC633895	LC633921	LC633934	LC633908
	SJB462	South Korea	*Fragaria* x *ananassa*	LC633896	LC633922	LC633935	LC633909
F. oxysporum f. sp. *melonis*	NRRL26406		*Cucumis melo*		LS479647	LS479201	
F. oxysporum f. sp.*pisi*	NRRL37622		*Cicer* sp.		LS479649	LS479203	
F. oxysporum f. sp.*raphani*	NRRL54005				LS479649	LS479203	
F. proliferatum	NRRL62905				KU171727	KU171707	
F. solani	NRRL32810	USA		DQ094577	DQ247118	EU329624	
F. solani (present isolates)	SJB62	South Korea	*Fragaria* x *ananassa*	LC633897	LC633923	LC633936	LC633910
	SJB222	South Korea	*Fragaria* x *ananassa*	LC633898	LC633924	LC633937	LC633911
	SJB243	South Korea	*Fragaria* x *ananassa*	LC633899	LC633925	LC633938	LC633912
F. solani f. sp. *batatas*	NRRL22400	USA	*Ipomoea batatas*	DQ094303	AF178343	EU329509	
F. solani f. sp. cucurbltae	NRRL22153		*Cucurbitae*	DQ094302	AF178346	EU329492	
F. solani f. sp. *mori*	NRRL22157	Japan	*Morus alba*	DQ094306	AF178359	EU329493	
F. solani f.s p. *robiniae*	NRRL22161	Japan	*Musa rubinea*	DQ094311	AF178330	EU329494	
F. solani f. sp. *xanthoxyli*	NRRL22163			AF178394	AF178328	EU329496	

Species	Isolates	Origin	Host	GenBank accession number			
				ITS	EF-1 α	rpb2	LSU
Fusarium sp.(FSSC24a)	NRRL32751	USA		DQ094531	DQ247070	EU329611	
Fusarium sp. (FSSC34)	NRRL46703			EU329712	HM347126	EU329661	
Fusarium sp. (FSSC9a)	NRRL32755	USA		DQ094534	DQ247073	EU329613	
Fusarium sp. (FSSC8)	NRRL43467	USA		EF453092	EF452940	EF469979	
Plectosphaerella alismatis	*CBS 113362*	Netherland		*LR026794*	*LR026489*	*LR026196*	*LR025932*
P. citrullae	*CBS 131741*	Netherland		*LR026796*	*LR026491*	*LR026197*	*LR025934*
P. cucumerina	*CBS 137.33*	Netherland		*LR026797*	*LR026492*	*LR026198*	*LR025935*
	CBS 139.60	Netherland		*LR026799*	*LR026494*	*LR026200*	*LR025937*
	CBS 137.37	Netherland		*LR026798*	*LR026493*	*LR026199*	*LR025936*
	CBS 286.64	Netherland		*LR026800*	*LR026495*	*LR026201*	*LR025938*
P. cucumerina (present isolates)	SJB163	South Korea	*Fragaria* x *ananassa*	LC633900	LC633926	LC633939	LC6339103
	SJB183	South Korea	*Fragaria* x *ananassa*	LC633901	LC633927	LC633940	LC633914
	SJB263	South Korea	*Fragaria* x *ananassa*	LC633902	LC633928	LC633941	LC633915
	SJB271	South Korea	*Fragaria* x *ananassa*	LC633903	LC633929	LC633942	LC633916
P. delsorboi	*CBS 116708*	Netherlan		*LR026810*	*LR026505*	*LR026209*	*LR025948*
P. guizhouensis	*CGMCC3.19658*	China		*MK880441*	*MK930453*	*MK930460*	*MK880431*
P. humicola	*CBS 423.66*			*LR026811*	*LR026506*	*LR026210*	*LR025949*
P. oligotrophica	*CBS 440.90*			*LR026814*	*LR026509*	*LR026211*	*LR025952*
P. pauciseptata	*CBS 131745*			*LR026816*	*LR026511*	*LR026212*	*LR025954*
P. plurivora	*CBS 260.89*			*LR026819*	*LR026514*	*LR026213*	*LR025957*
	CBS 292.66			*LR026822*	*LR026517*	*LR026214*	*LR025960*
	CBS 386.68			*LR026823*	*LR026518*	*LR026215*	*LR025961*
	CBS 642.63			*LR026826*	*LR026521*	*LR026216*	*LR025964*
P. ramiseptata	*CBS 131743*			*LR026831*	*LR026529*	*LR026224*	*LR025969*
P. nauculaspora	*CGMCC3.19656*	China		*MK880439*	*MK930451*	*MK930458*	*MK880424*
Brunneochlamydosporium nepalense	*CBS 277.89*			*LR026683*	*LR026385*	*LR026111*	*LR025812*

Multilocus phylogenetic analysis and species recognition

The obtained individual consensus sequences from *Fusarium* spp. were blasted against the Fusarium MLST database, and those obtained from *Plectosphaerella* spp. were blasted against GenBank to determine the closest matching species and species complex. Fungal species similar to the new isolates were used in phylogenetic analysis. Selected gene sequences of *Fusarium* spp. and *Plectosphaerella* spp. were downloaded from GenBank. All the fungal strain used in phylogenetic analysis are listed along with assigned GenBank accession numbers in Table 2. Individual gene sequences from the isolates belonging to the same genus were aligned using MEGA v.6.06 software (Tamura et al., 2013). The aligned sequences of Multiple genes/loci were concatenated in Mesquite v.2.75 (Maddison & Maddison 2011). First, the single alignment of *ITS*, *LSU*, *EF-1 α*, and *rpb*2 genes of *Fusarium* spp. isolates were used for phylogenetic analysis using the Fusarium MLST database. Second, a concatenated sequence of *EF-1 α*, and *rpb*2 genes were used for phylogenetic inference based on two independent algorithms—Bayesian analyses (BI) and maximum likelihood (ML). Regarding *Plectosphaerella* spp. isolates, phylogenetic

analysis based on BI and ML independent algorithms was conducted using a concatenated data set of *ITS*, *LSU*, *EF-1 α*, and *rpb*2. Mr Model Test v.2.3 (Nylander, 2004) was used for the best fit model. BI was run in Mr Bayes v.3.2.2 and ML in MEGA v.6.0 (Rorquist et al., 2012; Tamura et al., 2013). BI analysis included a Markov Chain Monte Carlo algorithm of four chains, with a stop rule option (split frequencies were below 0.01), and a tree was saved every 1000 generations. The 50% majority rule consensus trees and posterior probabilities (PP) were determined from the 75% held phylogenies after discarding 25% of the samples as the burn-in phase. The resulting trees were visualized using FigTree v.1.4.2 and MEGA v.6.0. For ML analyses, the bootstrap method (1000 replication), Tamura-Nei model, uniform rate, completed deletion and nearest-neighbor-interchange were used as default options.

Morphological characterization

Morphological characteristics of two representative isolates from each species were observed on PDA, oat-meal ager (OA), malt-extract agar (MA), corn-meal agar (CA), and V8 media after incubation at 25°C under 16 h light/8 h dark cycle. The fungal block (5mm) from the seven-day culture on PDA was transferred to the respective media. Each isolate was culture on three plates (90-mm petri dish) per media and two perpendicular measurements of colony diameter were determined every day for five-days. The size and shape of conidia, microconidia, macroconidia, chlamydospores, and conidiophores were examined and measured after mounting fungal structures slide glass in sterile water using light microscopy (Olympus BX43 microscope) at 400× magnification. The average and standard deviation were determined based on the measurement of 50 randomly selected conidia, microconidia, macroconidia, chlamydospores, and conidiophores each. Mycelial growth at various temperatures was evaluated. Mycelial block of approximate size 5 × 5 mm were cut from the actively growing margin of the seven-day old culture on PDA, transferred on 90-mm petri dish containing 25-ml PDA, and then incubated at 15°C, 18°C, 22°C, 25°C, 28°C, 30°C, 32°C, and 35°C in complete darkness. The single-trial consisted of three PDA plates per isolate per temperature. The colony diameter was measured as described above.

Pathogenicity assay

For the pathogenicity test, strawberry seedlings (cultivars) were collected from the greenhouse and transplanted in a pot containing autoclaved pit soils. After transplanting, seedlings were placed in a growth chamber at 25°C and under 16 h/8 h light/dark cycle and were watered regularly. The runner came out from the established plant. New strawberry plants were propagated by pegging down plantlets at the end runners into pots containing autoclaved pit soils. The plantlets were cut to free from the mother plant when they started to grow new leaves after approximately one month and were used for pathogenicity test. After seven days of -post-detaching from the mother plant, the plantlets were removed from pots, and the potting mixture was extracted from roots (shaking or with hand). Then, 10 replicate plants per species/inoculum were inoculated by dipping the source up to the crown in 500 mL of conidial suspension ($2 × 10^6$ conidia ml^{-1}) for 24 h in the dark. The conidial rest was prepared according to the aforementioned procedure. The same replicated control plants (10) per experiment were treated by dipping the root up to crown in 500-ml sterile deionized water for 24 h in the dark. After either inoculation or treatment, Strawberry plants were transplanted in the pot filled with the autoclaved potting mixture (pit soils: sand = 4:2), maintained in a growth chamber at 25°C and under 16 h/8h light/dark cycle, and irrigated daily with sterile water. Plants were monitored frequently to discover symptomatic plantlets.

Affected plantlets were further evaluated by observing the presence of root rot and discoloration inside the crown. Subsequently, the pathogen was reisolated and reidentified based on morphological characteristics and the sequence data of *rpb2* gene. Disease incidence (DI) was estimated as the proportion of symptomatic plantlets compared with the total number of inoculated plantlets.

Statistical analyses

The optimum temperature for the mycelial growth rate of the identified fungal species was estimated via nonlinear regression analysis using Gaussian four-parameter process in SigmaPlot v.14 (Systat Software, San Jose, CA). The mean and standard deviation (SD) of data were estimated using MS Excel. The growth rate of mycelium on various culture media was analyzed via ANOVA using SAS v.9.4, and lsd test was used to test for significant differences among or between different treatments at $P < 0.05$.

Results

Fungal isolation

Thirty isolates were obtained from rotten tissue of the crown and root of ~ 25 affected strawberry plants collected from different greenhouses in Sangju, South Korea. Most of these isolates were *Fusarium* spp. (22 isolates) and the rest were *Plectosphaerella* spp. (eight isolates). Among the isolates belonging to *Fusarium* spp., the colony of majority isolates was pinkish-white (16 isolates), whereas the settlement of reaming hermits was creamy or off white (six isolates).

Multilocus phylogenetic analysis

The multigene sequences from *Fusarium* spp. and *Plectosphaerella* spp. were subjected to phylogenetic analysis separately. The first phylogenetic tree illustrates the phylogenetic analysis among the *Fusarium* species, and the second one was among the *Plectosphaerella* spp. As the sequences of *ITS,LSU*, *EF-1 α*, and *rpb*2 were not available for all reference isolates, separate phylogenetic analysis was conducted using individual sequence data. In this case, unique gene sequences of reference *Fusarium* spp. were obtained from Fusarium MLST and GeneBank database. The present isolates were clustered into two separate clades (*F. oxysporum* species complex and *F. solani* species complex) consistently in the individual pyogenesis. The sequences of *EF-1 α*, and *rpb*2 are believed to the more informative for *Fusarium* spp. identification. Thus, the concatenated sequence of *EF-1 α*, and *rpb*2 were used to construct the multigene phylogenetic tree. Thirty-one representative *Fusarium* isolates, including the isolates from the current study and *Brunneochlamydosporium nepalense* as outgroup, were used to build the phylogenetic tree based on *EF-1 α*, and *rpb*2 sequence data. The concatenated sequences data set comprised 1231 total characters, including gap. In BI, 50% majority rules consensus tree with PP (Fig. 2) was estimated from the remaining 3920 trees after 1307 trees were discarded as the "burn-in" phase. Maximum likelihood analysis based on the Tamura-Nei model yielded the best ML tree with maximum log-likelihood of − 4062.0432. Codon positions included were 1st + 2nd + 3rd + noncoding, and there were a total of 733 places in the final dataset. Phylogenetic inference shows the position of all selected *Fusarium* isolate (nine isolates) (Fig. 2). Of these nine isolates, six were clustered in the *F. oxysporum* species complex and three in the *F. solani* species complex. The *F. oxysporum* species complex clade and three in *F. solani* species complex were highly supported (PP = 1; BS ≥ 90 %).

For the identification of *Plectosphaerella* spp., the multigene phylogenetic tree was constructed using the concatenated sequences of *ITS*, *LSU*, *EF-1 α*, and *rpb*2. The analysis involved 21 representatives *Plectosphaerella* isolates, including the isolates from the current study and one *Brunneochlamydosporium nepalense* CBS 277 89 (used as outgroup). The concatenated sequences dataset consists of 2400 characteristics, including gaps. The BI ended after 1 million generation, 50% majority rules consensus tree with PP (Fig. 3) were estimated from 1085 trees left after the 272 trees were discarded as the burn-in phase. Maximum likelihood analysis yielded the best ML tree with maximum log-likelihood of − 6629.1611. The ML alignment matrix had 2307 positions in the final dataset, and the coding positions included were 1st + 2nd + 3rd + noncoding. The Tamura-Nei model was used to run the full likelihood analysis. The phylogenetic tree revealed the work of the isolates obtained in this study (Fig. 3). All the isolates clustered with reference isolates of *P. cucumerina*. The clade of *P. cucumerina* is highly supported by the posterior probability and bootstrap value (PP = 1; BS = 98 %).

Morphological characterization

Based on the molecular analysis, it was confirmed that the isolates obtained from the affected strawberry with crown and root rot from the five greenhouse belong to *F. oxyporum* species complex, *F. solani* species complex, and *P. cucumerina*. The morphological characteristics of representative isolate of identified fungal species described in detail.

Morphological characterization of F. oxyporum species complex

The colony and culture of *F. oxyporum* species complex isolate are shown in Fig. 3. The comparison of morphological characteristics of present and reference isolates of *F. oxyporum* species complex shown in Table 3. The colony of present isolate (SJB593) on PDA was white and purple, whereas the colony of reference isolate (CBS 144134) was vinaceous. The shape of macroconidia and chlamydospore of the present isolate match those of reference isolate described by Lombard et al. (2019). The present isolate produced cylindrical microconidia, whereas connection isolate produced ellipsoidal to falcate microconidia. The average size microconidia (11.2 × 3.9 μm) and chlamydospore (12.0 × 11.1 μm) of the present isolate were slightly bigger than that microconidium (11.0 × 3.0 μm) and chlamydospore (≤ 10 μm diameter) of reference isolate. The average size of macroconidia of the present isolate was 26.1 × 4.7 μm, which is slightly smaller than that of macroconidia (28.7 × 5 μm) of reference isolate.

Table 3
The comparison of morphological data including colony, macroconidia, and microconida for present and reference isolates of *Fusarium* spp.

Features		*Fusarium oxysporum* species complex		*Fusarium solani* species complex	
		Present isolate (SJB593)	Reference isolate (CBS 144134) (Lombard et al. 2019)	Present isolate (SJB222)	Reference isolate (Yadou7-6) (Chang et al. 2018)
Colony on PDA		White, fluffy colonies and purple on the back	Vinaceous, floccose with abundant aerial mycelium	White colonies, reverse creamy white	Pale yellowish colonies, reverse yellowish
Microconidia	Shape	Cylindrical and tapering toward the end	Ellipsoidal to falcate	Cylindrical, curve or straight with blunted ends	—
	Size	8.3–16.3 × 3.0–4.8 µm (mean ± SD = 11.2 ± 1.9 × 3.9 ± 0.6 µm)	6.0–15.0 × 2.0–4.0 µm (mean = 11.0 × 3.0)	9.7–17.3 × 3.4–8.3 µm (mean ± SD = 12.9 ± 2.3 × 4.9 ± 0.9 µm)	—
Macroconidia	Shape	Mostly falcate, septa 2–5	Falcate, septa 1–5	Falcate, septa 3–6	Cylindrical, falcate, septa 3
	Size	22.0–35.3 × 3.9–5.6 µm (mean ± SD = 26.1 ± 3.2 × 4.7 ± 0.5 µm)	22.0–38.0 × 4.0–5.0 µm (mean = 28.7× 5 µm)	26.6–45.5 × 4.5–8.8 µm (mean ± SD = 33.0 ± 4.8 × 6.5 ± 1.1 µm)	25–30.2 × 4.1–4.6 µm (mean ± SD = 27.2 ± 1.9 × 4.3 ± 0.2 µm)
Chlamydospore	Shape	Globose	Globose to subglobose	Globose,single or in pair	—
	Size	8.6–15.7 × 7.6–14.3 µm (mean ± SD = 12.0 ± 2.1 × 11.1 ± 1.9 µm)	5–10 µm diam	6.8–10.9 × 6.6–11.6 µm (mean ± SD = 9.2 ± 1.2 × 8.7 ± 1.2 µm)	—

Morphological characterization of F. solani species complex isolate

Colony and microscopic characteristics of present isolate belonging to *F. solani* species complexes are shown in Fig. 5. The morphological characteristics, including colony color, shape, and size of microconidia, macroconidia, and chlamydospore of presents isolate, were comparable with those of reference isolate described by Chang et al. (2018) (Table 3). The colony color of the present isolate (SJB222) was white from up and creamy white from the reverse side, whereas Chang et al. (2018) described the colony color of the isolate (Yadou7-6) as a pale yellowish and yellowish on the back. The shape of macroconidia produced in present isolates is consistent with the shape of macroconidia of reference isolate. The present isolates had bigger macroconidia (33.0 × 6.5 µm) than that of the reference isolate. Miroconida of present isolates were cylindrical, curve, or straight and were 9.7–17.3 × 3.4–8.3 µm in diameter. The chlamydospore produced by the present isolate were globose, pair form, and were 6.8–10.9 × 6.6–11.6 µm in diameter.

Morphological characterization of P. cucumerina isolate

The colony and culture of *P. cucumerina* are shown in Fig. 6. The comparison of morphological characteristics of present and reference isolate of *P. cucumerina* are shown in Table 4. The morphological characteristics of the present isolate are comparable with that of the reference isolate of *P. cucumerina* (CBS131739) described by Carlucci et al. (2012). The colony of the present isolate was creamy white and pale yellowish from the reverse side. Conidiophores were simple (rarely branched) and were 10.6–44.9 × 2.2–5.4 µm in diameter. Conidia were ellipsoidal, tapered or rounded ends, guttate, 0–1 septate, and 8.5–13.1 × 3.2–6.4 µm in diameter. On average, the conidial size of present isolates was bigger than that of reference isolates. Carlucci et al. (2012) described the conidial size of *P. cucumerina* (CBS131739) as 7–10.5 × 2.5–3.5 µm (mean ± SD = 8.8 ± 1.3 × 2.8 ± 0.4 µm) in diameter.

Table 4
The comparison of morphological data, including colony, mycelium, conidiophore, and conidia for present and reference isolates of *P. cucumerina*.

Features		*Plectosphaerella cucumerina*	
		Present isolate (SJB271)	Reference isolate(CBS 131739) (Carlucci et al.2012)
Colony on PDA		Creamy white colonies, reverse pale yellowish	Various shades of buff to salmon pink
Mycelium		Hyaline, septate, branched, forming hyphal coils, 2.5−5.2 µm (mean ± SD = 4.2 ± 0.9 µm) wide.	Hyaline, septate, branched, forming hyphal coils
Conidiophore	Shape	Simple or rarely branched	Solitary, unbranched or rarely irregularly branched
	Size	10.6−44.9 × 2.2−5.4 µm (mean ± SD = 26.9 ± 11.3 × 3.3 ± 0.8 µm)	—
Conidia	Shape	Ellipsoidal, tapered or rounded ends, guttulate, 0−1 septate	Ellipsoidal, tapering gradually to rounded apex and base, guttulate, 0−1 septate
	Size	8.5−13.1 × 3.2−6.4 µm (mean ± SD = 10.6 ± 1.3 × 4.3 ± 0.7 µm)	7−10.5 × 2.5−3.5 µm (mean ± SD = 8.8 ± 1.3 × 2.8 ± 0.4 µm)

Effect of culture media and temperature on mycelial growth

The media have a significant influence on the mycelial growth rate (Fig. 7). The isolates of *F. solani* showed the highest growth rate on PDA, MEA, V8 and the least growth rate on CMA. In contrast, the isolates of *F. oxyporum* showed the best growth rate on V8 followed by CMA, OMA and the least growth rate on MEA. The growth rate of the isolate of *P. cucumerina* was significantly higher on V8 and CMA than on PDA, MEA, and OMA (Fig. 7A).The mycelium growth rate on the same culture media also depends on fungal species (Fig. 7B). For example, *F. oxyporum* grew significantly well on OMA followed by *F. solani* and *P. cucumerina*, whereas *F. solani* grew significantly better on MEA followed by *F. oxyporum* and *P. cucumerina*. *Plectrosporium cucumerina* showed poor growth rate on all tested media compared with that of *F. solani* and *F. Oxyporum* (Fig. 7B).The selected isolates representing each of the three fungal species were grown on PDA at 15°C−35°C. The maximum growth rate of *F. solani species complex* (isolate SJB222) was estimated at 25.2°C. In contrast, the top growth rates of *F. oxysporum species complex* (isolate SJB593) and *P. cucumerina* (isolate SJB271) were 22.0°C and 22.7°C, respectively (Fig. 8). *Plectrosporium cucamarina* exhibited the slowest growth rate at all tested temperature regimes. *F. solani* species complex (isolate SJB222) showed the highest growth rate at higher temperature (22.5°C−35°C), whereas *F. oxysporum* species complex showed at lower temperature (15°C−22.5°C).

Pathogenicity test

To confirm Koch's postulates, the pathogenicity of an identified representative isolate of *F. oxyporum* species complex (SJB593), *F. solani* species complex (SJB222), and *P. cucumerina* (SJB271) were tested by following the root dip assay method. The pant showed typical crown and root rot symptoms after 15 (*Fusarium* spp.) and 18 (*P. cucumerina*) days of inoculation (Fig. 9). The symptoms include wilting, root rot, and discoloration inside the crown, which was similar to those observed naturally infected plantlet in greenhouse. But tested isolate showed a different level of aggressiveness intern of DIs. The hermit of *P. cucumerina* showed the highest virulence with 80% DI followed by *F. solani* species complex with 70% and *F. oxyporum* species complex with 60% DI. The control plant remains healthy and asymptomatic (Fig. 9).

Discussion

The crown and root rot disease is a significant threat to strawberry production worldwide (Fang et al., 2011). According to the grower at Sangju, South Korea, the level of the crown and root rot in strawberry greenhouse increase in the late production season. Low pH levels (4.5−6) influence the outbreak of this disease (Fang et al., 2011). Three fungal species were recovered from the deceased strawberry crown and were discerned as *F. oxyporum* species complex, *F. solani* species complex, and *P. cucumerina* based on distinct molecular and morphological characteristics. The pathogenicity assay revealed that the isolates of these fungal species reproduced identical disease symptoms. Therefore, this study concluded *F. oxyporum* species complex, *F. solani* species complex, and *P. cucumerina* are responsible for

the crown and root rot of strawberry in Sangju, South Korea. *F. oxyporum* species complex were the most reported fungal species that cause crown and root rot of strawberry, but this is the first report showing *F. solani* species complex and *P. cucumerina* as the causative agent of this disease. Proper diagnosis of this new pathogen is crucial because early identification and disease monitoring are the most important critical steps for implementing any disease management program (Riley et al., 2002).

With the progress in molecular analysis and bioinformatics, the crystal explicit knowledge regarding fungi and their association with the host has increased over the last decade (Chung et al., 2020). The multigene phylogenetic approach uses sophisticated and reliable tools for the classification of cryptic fungal taxa and fungi, including plant pathogen. The filamentous fungal genus *Fusarium* is one of the most destructive plant pathogen comprised of 300 phylogenetically distinct species distributed among ~ 23 species complex (O'Donnell et al., 2015; Dongzhen et al., 2020). Initially, fungal species within the *Fusarium* genus were identified based on iconic fusiform multiseptate macroconidia. The morphological and morphological phylogenetic studies revealed that they convergently evolved into different lineages of ascomycetes (O'Donnell et al., 2015). So, the use of molecular markers (DNA sequences) is more reliable for identifying closely related species. In this study, we identified *F. oxyporum* and *F. solani* species complex based on phylogenetic inference using concatenated sequences of *EF-1 α*, and *rpb*2. The sequences of *EF-1 α* and *rpb*2 highly recommend for phylogenetic analysis and BLASTn against curated reference sequences in the FUSARIUM-ID and Fusarium MLST database for identification to assess species-level identification within the genus *Fusarium* (O'Donnell et al., 2015; Šišić et al., 2018). In this study, these loci showed high potential to distinguish the different *Fusarium* species complex, including the *F. oxyporum* and *F. solani* species complex.

Plectosporium was first described in 1995 as the new genus for the species previously known as *Fusarium tabacinum* (*Cephalosporium tabacinum*), the anamorph of *Plectosphaerella cucumerina* (Palm et al., 1995). Some studies recommend using *LSU*, *ITS*, *EF1α*, and *RPB2* sequences data to resolve the taxonomy of the *Plectosphaerella* species (Giraldo & Crous 2019; Zhang et al., 2019). This study also found that the concatenated sequences of these loci are very informative for identifying *P. cucumerina*.

The morphological characteristics of identified fungal species in this study were comparable with that of the respective reference species and species complex (Tables 3 and 4). This study found that there are some differences in morphological characteristics; for example, macroconidia of the present isolate of *F. oxyporum* species complex (SJB 593) were smaller than that of reference isolate (CBS 144134), whereas macroconidia of the present isolate of *F. solani* species complex (SJB222) were larger than that of reference isolate Yadou7-6 (Table 3). The conidia of *P. Cucumerina* also isolates are larger than that of reference isolate CBS 131739. The slight morphological differences within the same species are explained by the difference in host, geographical location, and cultural condition. Many studies reported that morphological characteristics fungal species are influenced by the host, geographical location, culture media, and cultural condition (Stewart et al., 2006; Weir et al., 2012; Hassan et al. 2018). This study also found that *F. oxyporum* species grew well on PDA and V8 and *F. solani* and *P. cucumerina* on V8 and CMA. So, V8 could be the best choice to culture these species.

Among the fungal species, *Fusarium* species exhibited greater mycelial growth in warm temperature (Fig. 8). The adaptability of *Fusarium* species in warm temperature explain its current geographical distribution. Warm and rainfall are the favorable condition for *Fusarium* species to infect crops (Doohan et al., 2003). In contrast, the favorable condition for *P. cucumerina* were high humidity and low temperature (20°C–26°C) (Gilardi et al., 2012).

In general, both *Fusarium* species (*F. oxyporum* and *F. solani*) soil in-habiting species capable of causing disease, including wilt, root rot and crown rot of all economically important crops. In South Korea, *F. oxyporum* has been reported as the causative agent for wilt of many plant species, including prickly lettuce, larch, and chrysanthemum (Kwon et al., 2013; Hassan et al., 2019; Kim & Choi 2020). In contrast to *F. oxyporum*, *F. solani* is not a frequently reported fungal species in South Korea. It has been reported as the causative agent wilt of cucumber coastal hog fennel and sweet potato (Han et al., 2012; Yang et al., 2018; Kwon et al., 2020). To the best of our knowledge, *F. solani* has not been reported as the causative agent of crown and root rot of strawberry in South Korea. Like *Fusarium* spp., *P. cucumerina* also soil inhabiting plant pathogen and has been reported on many crops, including alfalfa, cabbage, potato, tomato, and sunflower (Abad et al., 2000; Li et al., 2017). Though having a wide host range, it was reported only on the wild arrowhead in South Korea (Li et al., 2017). To the best of our knowledge, this is the first report of root and crown rot of strawberry caused by *P. cucumerina* in South Korea.

Evolving of the new pathogen under existing cultural practices and control methods indicates that it is necessary to adopt new cultural practices and control strategies. Strawberry grower in Sangju use river water for irrigation. Inoculum of this disease may come through contaminated irrigated water. Plant debris of affected plant also a crucial source of inoculum. Plant debris was observed during the survey. This plant debris may be mixed with soil in pot mixture and infect the newly propagated plantlet. Proper disposal of affected plant debris is necessary. For developing chemical strategies to control this disease, a representative isolate of identified fungal taxa in this study needs to be tested for estimation of efficacy of traditional fungicides (benomyl, captan, mefenoxamand thiophanate methyl).

In conclusion, the finding of this study indicates essential information to develop sustainable control measures for crown and root rot of strawberry in South Korea.

Declarations

References

1. Abad, P., Pérez, A., Marqués, M. C., Vicente, M. J., Bruton, B. D.& García-Jiménez, J.(2000). Assessment of vegetative compatibility of *Acremonium cucurbitacearum*and *Plectosphaerella cucumerina* isolates from diseased melon plants. *Bulletin OEPP*, *30*(2), 199–204.
2. Carlucci, A., Raimondo, M. L., Santos, J. & Phillips, A. J. (2012). *Plectosphaerella* species associated with root and collar rots of horticultural crops in southern Italy. *Persoonia*, *28*, 34–48.
3. Chang, X., Dai, H., Wang, D. Zhou, H., He, W., Fu, Y., Ibrahim, F., Zhou, Y., Gong, G. Shang, J., Yang, J., Wu, X., Yong, T., Song, C. & Yang,W. (2018). Identification of *Fusarium*species associated with soybean root rot in Sichuan Province, China. *EurrpeanJournal ofPlant Pathology, 151*, 563–577.
4. Chung, P. C., Wu, H. Y., Wang, Y. W., Ariyawansa, H. A., Hu, H. P., Hung, T. H., Tzean, S. S. & Chung, C. L. (2020). Diversity and pathogenicity of Colletotrichum species causing strawberry anthracnose in Taiwan and description of a new species, *Colletotrichum miaoliense* nov. *ScientificReport*,*10*, 14664.
5. Dongzhen, F., Xilin, L., Xiaorong, C., Wenwu, Y., Yunlu, H., Yi, C., Jia, C., Zhimin, L., Litao, G., Tuhong, W., Xu, J. &Chunsheng, G. (2020). *Fusarium*Species and *Fusarium oxysporum* Species Complex Genotypes Associated With Yam Wilt in South-Central China. *Frontiers in microbiology*, *11*, 1964.
6. Doohan, F. M., Brennan, J. & Cooke, B. M. (2003). Influence of climatic factors on Fusarium species pathognic to cereals. *EurrpeanJournal ofPlant Pathology,109*, 755–768.
7. Fang, X. L., Phillips, D., Li, H., Sivasithamparam, K. & Barbetti, M.J. (2011). Severity of crown and root diseases of strawberry and associated fungal and oomycete patho- gens in Western Australia. *Australasian Plant Pathology40*, 109-119.
8. Fang, X., Phillips, D., Verheyen, G., Li, H., Sivasithamparam, K. & Barbetti, M. (2012). Yields and resistance of strawberry cultivars to crown and root diseases in the field, and cultivar responses to pathogens under controlled environment conditions. *Phytopathologia. Mediterranae,51*, 69-84.
9. Geiser, D. M., Jiménez-Gasco, M., Kang, S., Makalowska, I., Veeraraghavan, N., Ward, T. J., Zhang, N. Kuldau, G.A. &O'Donnell, K., (2004). FUSARIUM-ID v.1.0: A DNA sequence database for identifying *Fusarium*. *EurrpeanJournal ofPlant Pathology,110*, 473–479.
10. Gilardi, G., Bergeretti, F., Gullino, M. L.& Garibaldi, A. (2019). First Report of *Neopestalotiopsis clavispora* Causing Root and Crown Rot on Strawberry in Italy. *Plant disease,103*, 2959.
11. Gilardi, G., Ortu, G., Gullino, M. L.& Garibaldi, A. 2012. *Plectosphaerella cucumerina*: a new pathogen on wild rocket in Italy. *Protezione dele Colture*,*5*, 31-33. (Summery in English).
12. Han, K.S., Lee, S.C., Han, Y.K., Kim, D.H. & Kim, S. (2012). Crown and Foot Rot of Grafted Cucumber Caused by *Fusarium solani* sp. cucurbitae. *ResearchPlantDisease, 18*, 57–61.

13. Hassan, O. Lim, T.-H. & Chang, T. (2019). Damping-Off of Larch (Larix kaempferi) Caused by *Fusarium oxysporum*in Korea. *Plant Disease*,*103*, 1037-1037.

14. Hassan, O., Jeon, J. Y., Chang, T., Shin, J. S. & Oh, N. K. (2018). Molecular and morphological characterization of *Colletotrichum*species in the *Colletotrichum gloeosporioides* complex associated with persimmon anthracnose in South Korea. *Plant Disease*, *102*, 1015–1024.

15. Hellin, P, Scauflaire, J., Van Hese, V., Munaut, F. &Legrève, A. (2017). Sensitivity of *Fusarium culmorum* to triazoles: impact of trichothecene chemotypes, oxidative stress response and genetic diversity. *Pest management science*, *73(6), 1244–1252.*

16. Kim, B. R. and Choi, Y. J. 2020. *Fusarium fujikuroi*Causing Fusarium Wilt of Lactuca serriola in Korea. *Plant Disease*, *105*, 502-502.

17. (2009). The Korean Society of Plant Pathology. List of plant diseases in Korea. 5th ed. Seoul: Korean Society of Plant Pathology.

18. Kwon, J. H., Choi, O. &Kim, J. (2013). *Fusarium oxysporum* Causing Wilt and Stem Rot in Chrysanthemum × morifolium in Korea. *Plant disease*,*97*,

19. Kwon, S. K., Jeon, C.W. & Kwak, Y. S. (2020). First Report of Wilt Disease on *Peucedanum japonicum* and Selection of Fungicides. *The Korean Journal of Pesticide Science*,*24*, 7-13. (Abstract in English).

20. Li, P. L., Chai, A. L., Shi, Y. X., Xie, X. W. & Li, B. J. (2017). First Report of Root Rot Caused by *Plectosphaerella cucumerina*on Cabbage in China. *Mycobiology, 45*, 110–113.

21. Lombard, L., Sandoval-Denis, M., Lamprecht, S. C. & Crous, P. W. (2019). Epitypification of *Fusarium oxysporum* clearing the taxonomic chaos. *Persoonia*,*43*,1-47.

22. Maddison, W. P. and Maddison, D. R. (2011). Mesquite: a modular system for evolutionary analysis. Version 2.75. http://mesquiteproject.org.

23. Maryani, N., Lombard, L., Poerba, Y.S., Subandiyah, S., Crous, P.W. & Kema, G.H.J. (2019).Phylogeny and genetic diversity of the banana Fusarium wilt pathogen *Fusarium oxysporum* sp. *cubense* in the Indonesian centre of origin. *Studies in Mycology*,*92*, 155–194.

24. Nam, M. H., Kim, H. S., Park, M. S., Min, J. Y. and Kim, H. T. (2020). Genetic Diversity, Pathogenicity, and Fungicide Response of *Fusarium oxysporum* sp. *fragariae* Isolated from Strawberry Plants in Korea. *Research inPlant*Disease,*26*, 79-87.

25. Nylander, J. A. A. (2004). MrModelTest v2. Program Distributed by the Author. Uppsala, Sweden: Evolutionary Biology Centre, Uppsala University.

26. O'Donnell, K., Ward, T.J., Robert, V.A.R.G., Crous, P.W., Geiser, D. M. and Kang, S.(2015).DNA sequence-based identification of *Fusarium*: Current status and future directions. *Phytoparasitica, 43*, 583–595.

27. O'Donnell, K., Sutton, D. A., Rinaldi, M. G., Sarver, B. A., Balajee, S. A., Schroers, H. J., Summerbell, R. C., Robert, V. A., Crous, P. W., Zhang, N., Aoki, T., Jung, K., Park, J., Lee, Y. H., Kang, S., Park, B. & Geiser, D. M. (2010). Internet-accessible DNA sequence database for identifying fusaria from human and animal infections. *J Journal of clinical microbiology*,*48*, 3708–3718.

28. Palm, M. E., Gams, W. & Nirenberg, H. I. (1995). *Plectosporium*, a new genus for *Fusarium tabacinum*, the anamorph of *Plectosphaerella cucumerina*. *Mycologia*,*87*, 397–406.

29. Park, K., Han, I., Lee, S.-M., Choi, S.-L., Kim, M. C. & Lee, H. (2019). Crown and Root Rot of Strawberry Caused by *Neopestalotiopsis clavispora* in Korea.*TheKoreanJournal ofMycology*,*47*, 427–435. (Abstract in English).

30. Ramdial, H., De Abreu, K. & Rampersad, S. N. (2017). Fungicide Sensitivity among Isolates of *Colletotrichum truncatum*and *Fusarium incarnatum-equiseti* Species Complex Infecting Bell Pepper in Trinidad. *ThePlant PathologyJournal, 33*, 118–124.

31. Rehner, S. A.&Samuels, G. J. (1994). Taxonomy and phylogeny of *Gliocladium* analysed from nuclear large subunit ribosomal DNA sequences. *MycologicalResearch*,*98*, 625–634.

32. Riley, M.B., Williamson,M.R. & Maloy, O. (2002). Plant disease diagnosis. The Plant Health Instructor. DOI: 10.1094/PHI-I-2002-1021-01

33. Ronquist, F., Teslenko, M., van der Mark, P., Ayres, D.L., Darling, A., Höhna, S., Larget, B., Liu, L., Suchard, M. A.&Huelsenbeck, J.P. (2012). MrBayes 3.2: efficient Bayesian phylogenetic inference and model choice across a large model space. *Systematic biology*, *61*(3), 539–542.

34. Šišić, A., Al-Hatmi, A., Baćanović-Šišić, J., Ahmed, S. A., Dennenmoser, D., de Hoog, G. S. and Finckh, M. R. (2018). Two new species of the *Fusarium solani* species complex isolated from compost and hibiscus (Hibiscus sp.). *Antonie van Leeuwenhoek, 111*(10), 1785–1805.

35. Stewart, J. E., Kim, M.-S., James, R. L., Dumroese, R. K. & Klopfenstein, N. B. (2006). Molecular characterization of *Fusarium oxysporum* and *Fusarium commune* isolates from a conifer nursery. *Phytopathology*,*96*,1124-1133.

36. Surovy, M.Z., Kabir, M.K., Gupta, D. R., Hassan, O., Mahmud, N.U., Sabir, A.A., Rahman, M., Chang, T., Panaccione, D. G. & Islam, M. T. (2019). First report of *Fusarium* wilt caused by *Fusarium oxysporum* on strawberry in Bangladesh. *Plant Disease*,*103*, 367–368.

37. Tamura, K., Stecher, G., Peterson, D., Filipski, A. & Kumar, S. (2013). MEGA6: Molecular Evolutionary Genetics Analysis Version 6.0. *Molecular biology and evolution*, *30*(12), 2725–2729.

38. Taylor, J. W., Jacobson, D. J., Kroken, S., Kasuga, T., Geiser, D. M., Hibbett, D. S. & Fisher, M.C. (2000). Phylogenetic species recognition and species concepts in fungi. *Fungal genetics and biology : FG & B*, *31*(1), 21–32.

39. Vilgalys, R. and Hester, M. (1990). Rapid genetic identification and mapping of enzymatically amplified ribosomal DNA from several *Cryptococcus Journal of bacteriology*, *172*(8), 4238–4246.

40. Wei, H., Liu, C. & Ryong Jeong, B. (2020). An Optimal Combination of the Propagation Medium and Fogging Duration Enhances the Survival, Rooting and Early Growth of Strawberry Daughter Plants. *Agronomy*,10,

41. Weir, B. S., Johnston, P. R. &Damm, U. (2012). The *Colletotrichum gloeosporioides* species complex. *Studies in Mycology*,*73*, 115–80.

42. White, T.J. Bruns, T. &Taylor, J. (1990). Amplification and direct sequencing of fungal ribosomal RNA genes for phylogenetics. In: Innis MA, Gelfand DH, Sninsky JJ et al (eds) PCR protocols: a guide to methods and applications. Academic Press, San Diego, pp 315–322.

43. Yang, J. W., Nam, S. S., Lee, H. U., Choi, K. H., Hwang, S. G. & Paul, N. C. (2018). Fusarium root rot caused by *Fusarium solani*on sweet potato (Ipomoea batatas) in South Korea. *Canadian Journal ofPlantPatholology*, *40*, 90–95.

44. Zhan, Y.J., Peng, W.J., Xu, Z.Q., Xu, H. & Feng, X.H. First Report of *Phytopythium helicoides*Causing Root and Crown Rot on Strawberry in China. *Plant disease*,*104*,2528.

45. Zhang, Z. Y., Chen, W. H., Zou, X., Han, Y. F., Huang, J. Z., Liang, Z. Q.& Deshmukh, S. K. 2019. Phylogeny and taxonomy of two new *Plectosphaerella* (*Plectosphaerellaceae*, *Glomerellales*) species from China. *MycoKeys, 57*, 47–60.

Figures

Figure 1

Crown and root rot of strawberry;A–B: affected strawberry plants in green house;C: root and crown discoloration in wilted and collapse strawberry plant in green house;D: crown discoloration.
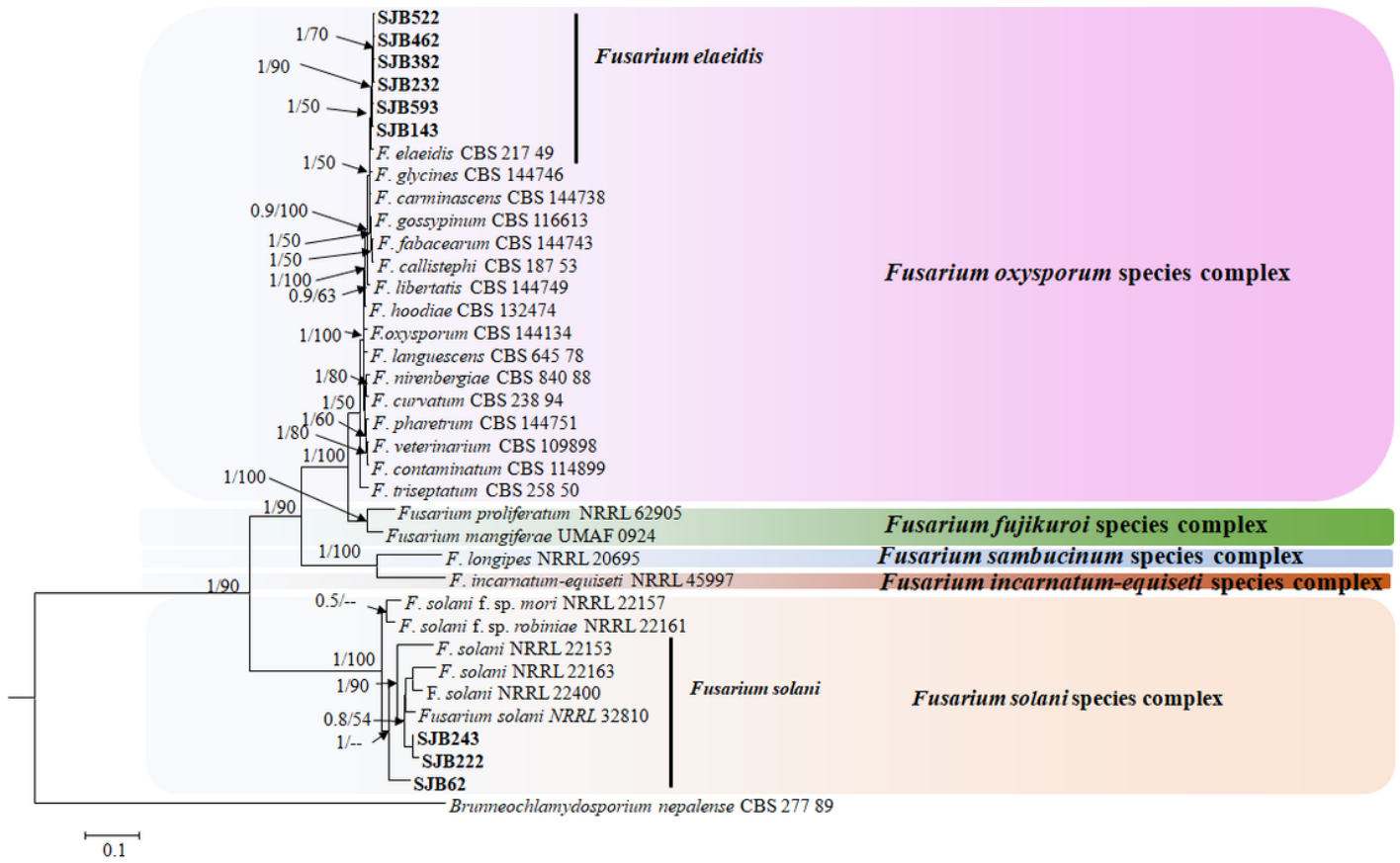
Figure 2

A Bayesian inference phylogenetic tree based on combined EF1-α and rpb2 sequence alignment of Fusarium spp. The present isolates are indicated in bold color. Bayesian posterior probability (PP ≥ 0.50), maximum likelihood bootstrap support values (ML ≥ 50)are shown at the nodes (PP/ML). The scale bar shows the expected number of substitutions per site.
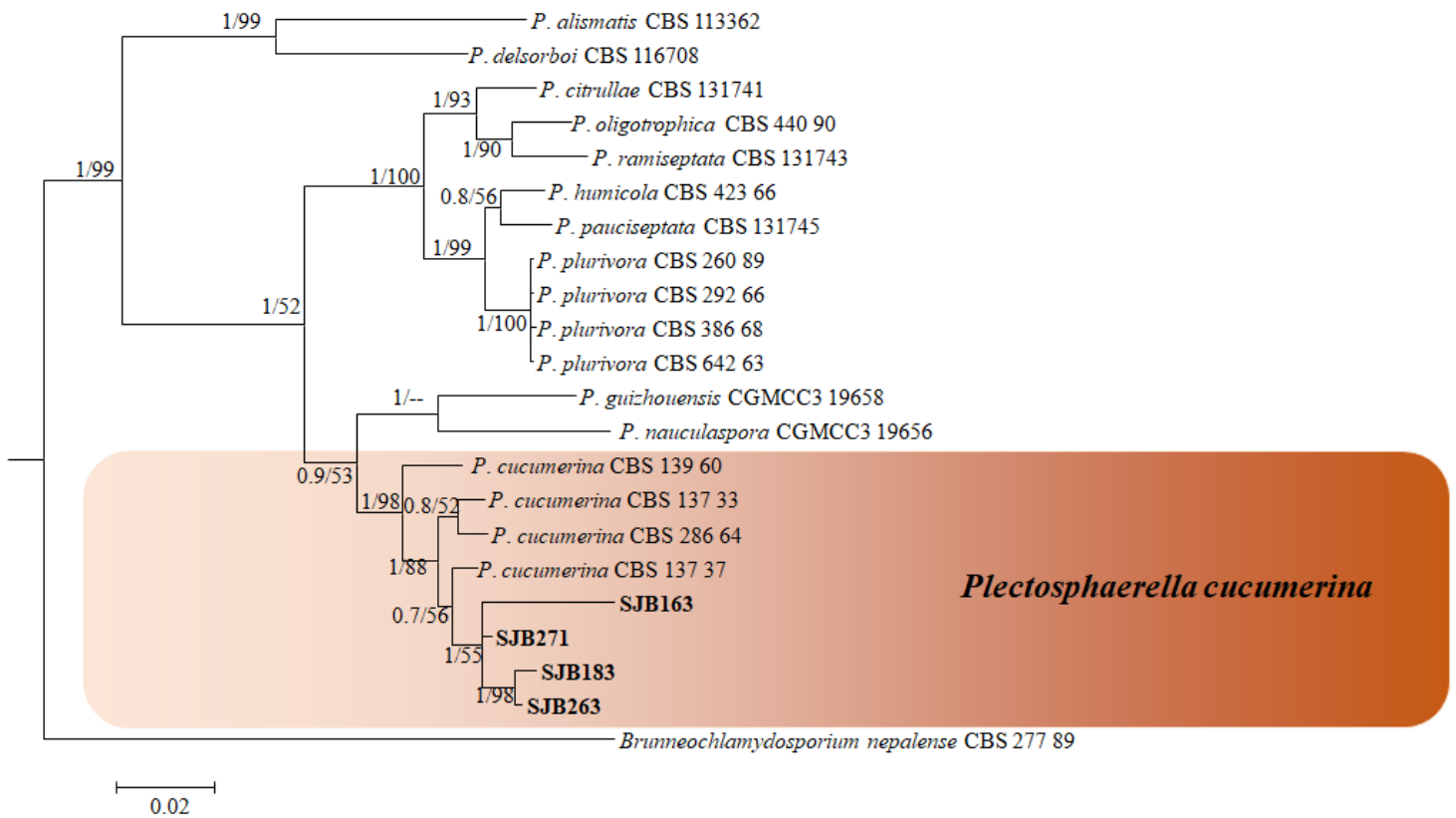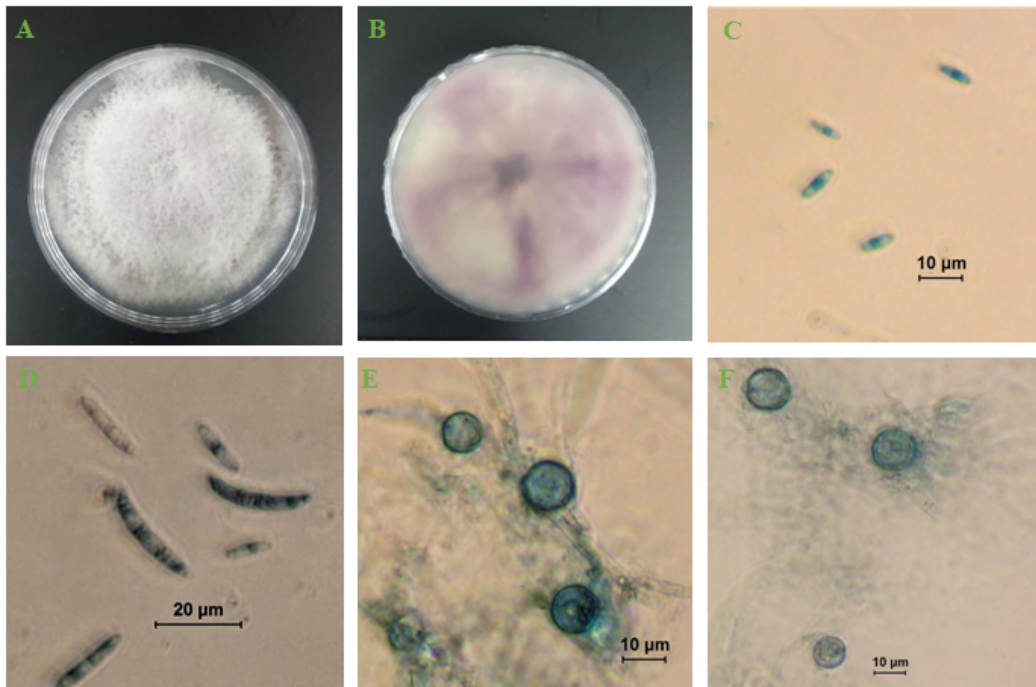
Figure 3

A Bayesian inference phylogenetic tree based on combined ITS, LSU, EF1-α, and rpb2 sequence alignment of Plectosphaerella spp. The present isolates are indicated in bold color. Bayesian posterior probability (PP ≥ 0.50), maximum likelihood bootstrap suport values (ML ≥ 50)are shown at the nodes (PP/ML). The scale bar shows the expected number of substitutions per site.

Figure 4

Morphological characteristics of Fusarium oxysporum species complex (isolate SJB593);A−B: Colony on PDA. C: Microconidia;D: Macroconidia;E−F: Clamidospore.

Figure 5

Morphological characteristics of Fusarium solani species complex (isolate SJB222);A−B: Colony on PDA;C: Microconidia;D: Macroconidia;E−F: Clamidospore.
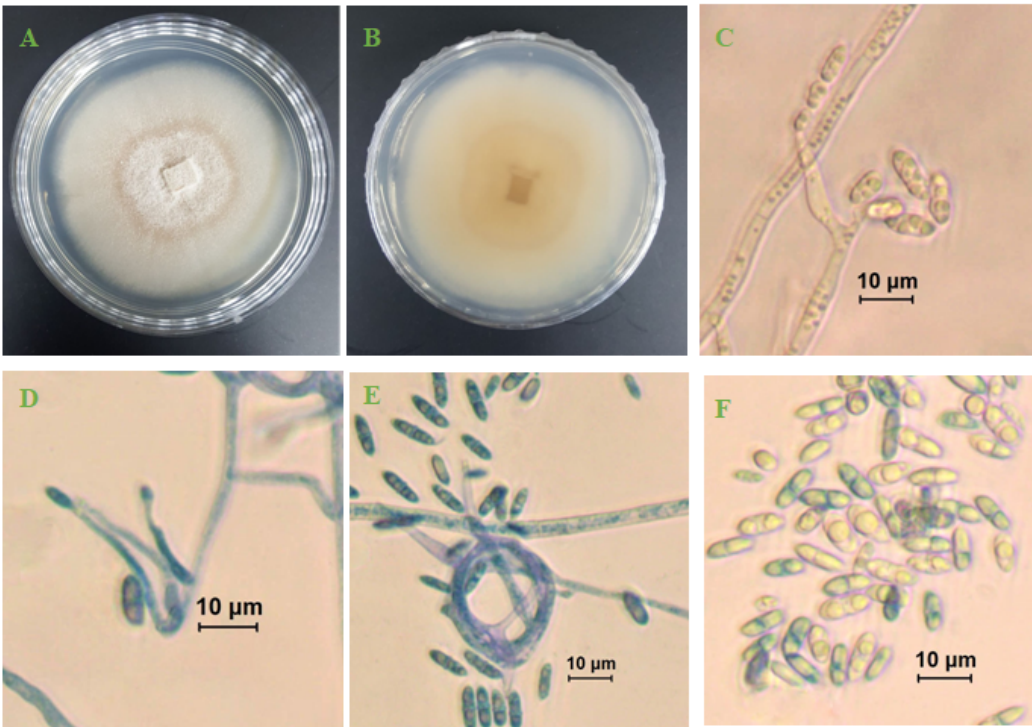

Figure 6

Morphological characteristics of Plectosphaerella cucumerina (isolate SJB271); A−B: Colony on PDA;C−D: Conidiophores and phialides;E: Hyphal coil and conidia;F: Conidia.

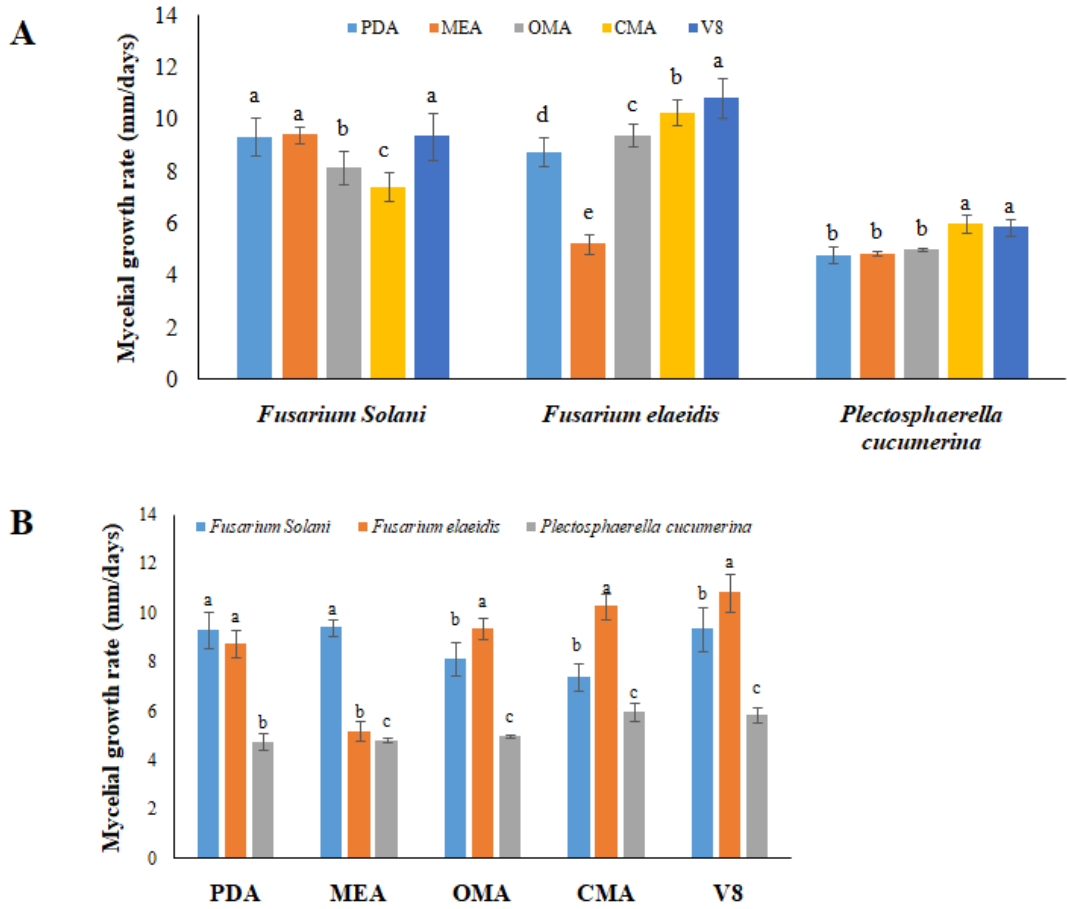**Figure 7**

Effect of culture media on mycelial growth;A: Mycelial growth of different fungal species on some media;B: Mycelial growth of some fungal species on different media.
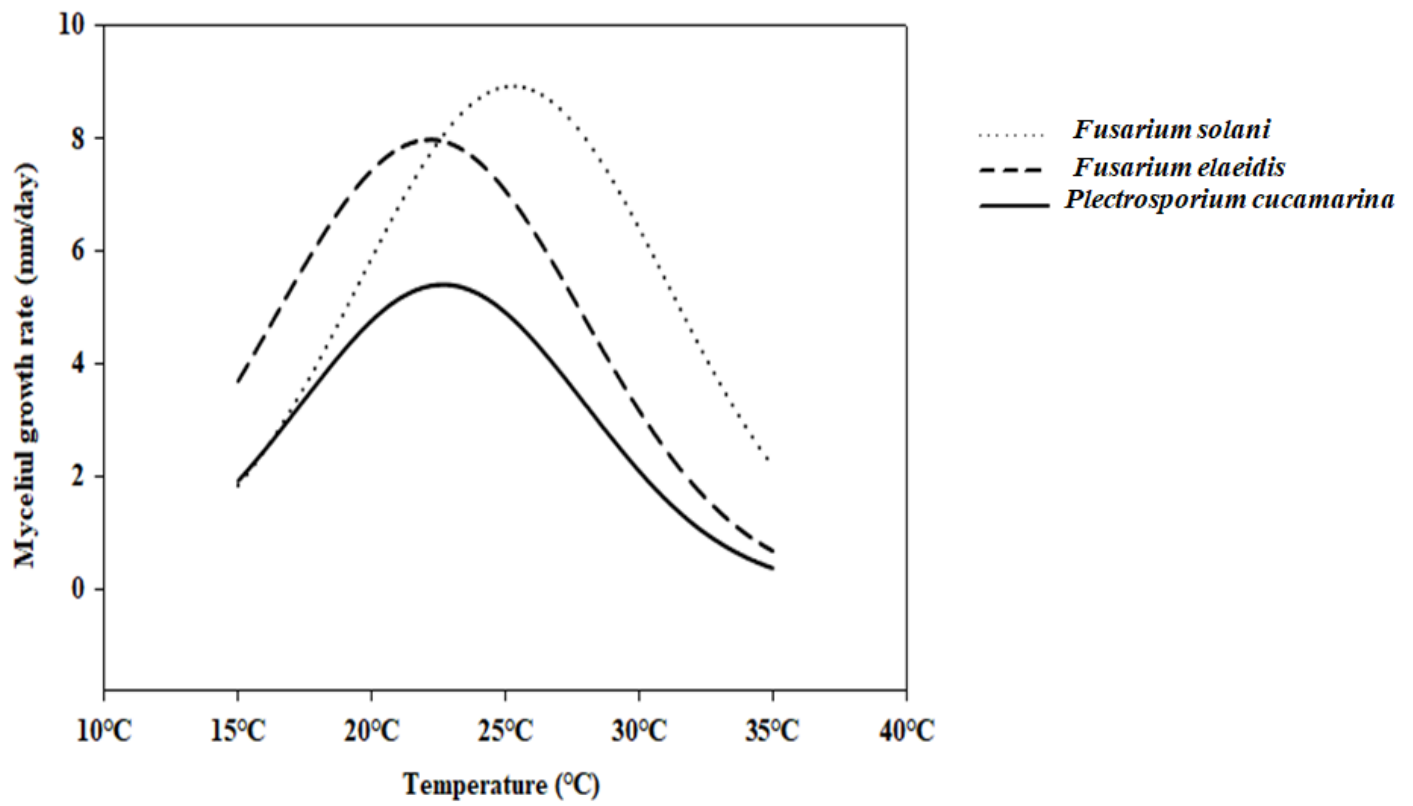
Figure 8

Mycelial growth rates of different fungal species at different temperatures. Gaussian process regression was used to estimate the optimum temperature for mycelial growth.
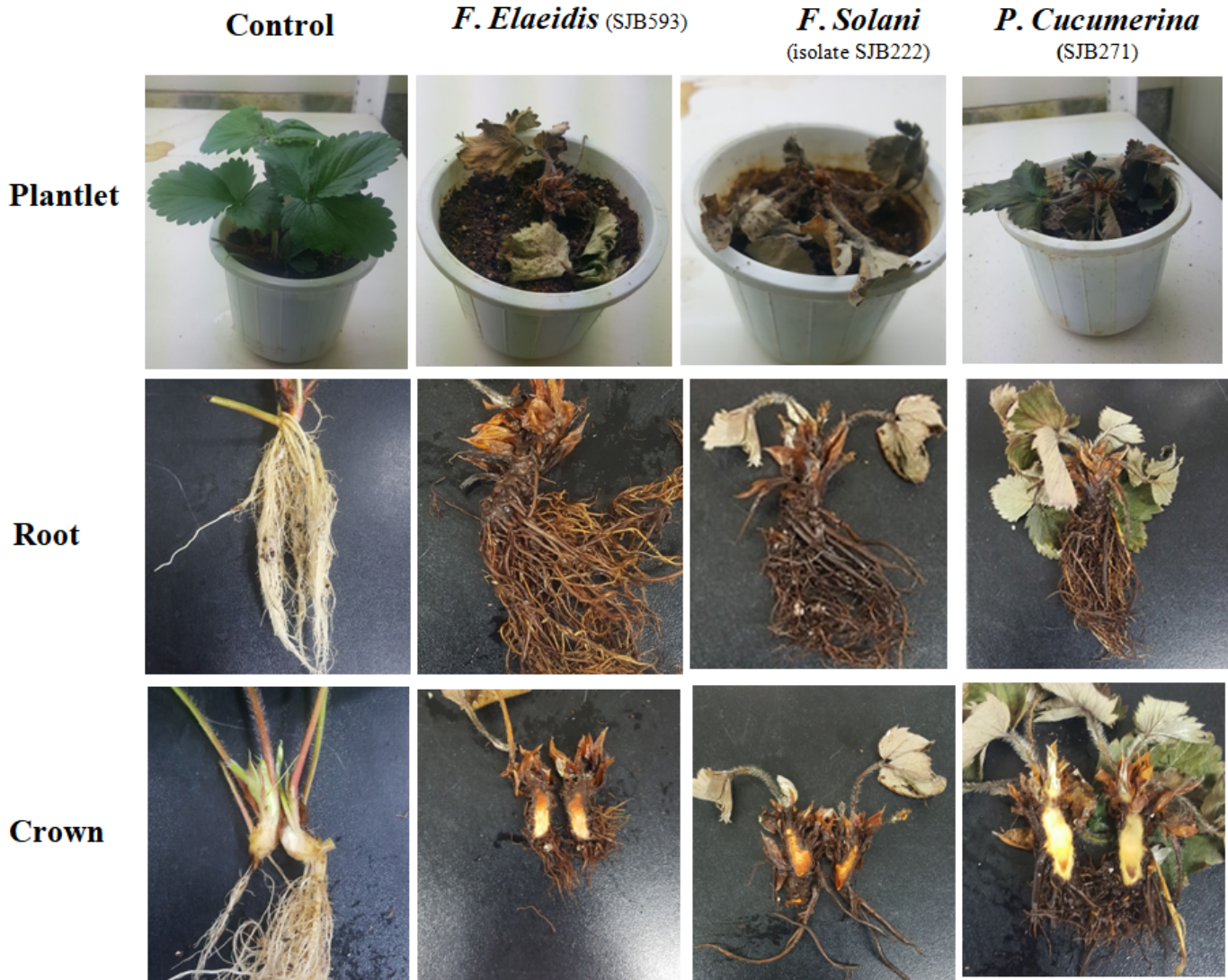
Figure 9

Symptoms showed by strawberry plantlets after inoculation with sterile water (control) and fungal speciesat 25°C and under 16h/8h light/dark cycle.